AIP | Applied Physics Letters

Nanoliter-sized overheated reactor

P. Neužil, W. Sun, T. Karásek, and A. Manz

Citation: Applied Physics Letters **106**, 024104 (2015); doi: 10.1063/1.4905851
View online: http://dx.doi.org/10.1063/1.4905851
View Table of Contents: http://scitation.aip.org/content/aip/journal/apl/106/2?ver=pdfcov
Published by the AIP Publishing

Nanoliter-sized overheated reactor

P. Neužil,[1,2,3] W. Sun,[2,4] T. Karásek,[5] and A. Manz[3]
[1]*CEITEC, Brno University of Technology, Antonínská 1, 602 00 Brno, Czech Republic*
[2]*Institute of Bioengineering and Nanotechnology, The Nanos, 31 Biopolis Way, Singapore 138669*
[3]*KIST-Europe, Campus E7.1, Saarbruecken D-66123, Germany*
[4]*Bruker Singapore Pte. Ltd., The Helios. 11 Biopolis Way, Singapore 138667*
[5]*IT4Innovations National Supercomputing Center, Studentská 6231/1B, 708 33 Ostrava, Poruba, Czech Republic*

(Received 3 October 2014; accepted 30 December 2014; published online 16 January 2015)

We report on a microfluidic system formed by 200 nl water droplets, encapsulated by a 600 nl mineral oil placed on a hydrophobically coated glass microscope cover slip. The micromachined heater underneath the glass was able to heat up the sample at a heating rate of 650 °C/s, heating the water sample up to 200 °C in less than 2 s. The sample/glass and the sample/oil interface did not have nucleation centers, showing that the sample reached a superheated stage without the necessity of being pressurized to suppress boiling. This method can be utilized for various applications currently being conducted in autoclaves.
[http://dx.doi.org/10.1063/1.4905851]

High temperature aqueous conditions are widely used in pressure cookers or autoclaves. The "steam digester" was an invention of the 17th century, commercially available since the 19th century, and available for home use since the late 1930s. The energy transfer is provided mainly by the heated steam. Its purpose is to reduce the related energy consumption and to shorten cooking time, i.e., the time needed for the denaturation of proteins and biological tissue. It has also been used for sterilizing food, for the so-called Maillard reaction used in food flavoring, and in the context of biological laboratories (autoclaving) or chemical synthesis (hydrothermal synthesis). Water normally starts to boil when its temperature is high enough for the vapor pressure to reach the external pressure level. Nucleation or surface tension effects are crucial because the expansion of very small vapor bubbles requires more force than that of larger ones. Indeed, warming water-based samples above 100 °C at a pressure of 1 bar could inevitably lead to boiling when nucleation sites are present, in places such as scratches on the surface.[1] In the absence of nucleation sites under the condition of uniform heating, the temperature of the liquid can exceed the boiling temperature in phenomena called superheating.[2] This phenomenon can result in water "explosions" rarely occurring in microwave ovens.

Starting in the last century, a popular separation technique for ions, DNAs/RNAs, and proteins called capillary electrophoresis was introduced. It is based on the flow of the fluid in a fused silica capillary with different internal diameters such as 5 μm, 50 μm, and 150 μm. The capillary is pulled from molten SiO_2 and due to surface forces during the solidification process; the internal surface of the capillary is scratch-free. Recently, we demonstrated this capillary-based system for spore breaking and releasing their DNA.[3] We were able to achieve a stable water-based system overheated up to a temperature of 240 °C for 30 min and supercooled down to −12 °C. The system required a syringe pump to force the sample to pass through the heated zone. The sample contained spores which had the tendency to sediment in the syringe, thus control spore concentration in the capillary itself was complicated and made reproducing the results a complicated task.

In our previous work,[4] we described a system called the virtual reaction chamber (VRC). It was formed by a sample droplet encapsulated by an immiscible mineral oil to eliminate sample evaporation placed on a hydrophobically coated glass microscope cover slip. Its cross section of two superposed droplets is shown in Fig. 1. The majority of the sample was in contact with oil and this liquid/liquid interface formed by two immiscible liquids obviously cannot contain nucleation centers. A small portion of the sample surface might be also in contact with glass with a high quality surface and no apparent mechanical scratches, i.e., also nucleation-centers free. Thus, the requirements for superheating of the sample were fulfilled. The water droplet had a volume of 0.2 μl with a near-spherical shape. A sphere of the same volume has a diameter of 0.73 mm.

In this paper, we report on the technical aspects of a nanoliter-sized system capable of superheating rapidly in

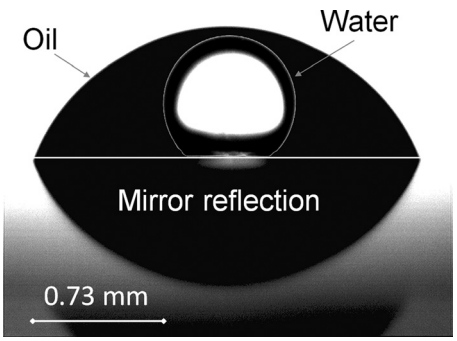

FIG. 1. Superimposed images of 200 nl water droplet over the profile of a 600 nl oil droplet, both placed on hydrophobic (contact angle 113°) and oleophobic surface (contact angle 77°). The contour of the sample droplet was added to increase the contrast for easier visualization.

less than 2 s water based samples to temperatures up to 200 °C. It is a simple system which could become a component of choice at the front-end of a lab-on-a-chip or micro total analysis system (μTAS) for spore disruption and subsequent DNA amplification by polymerase chain reaction (PCR) and its detection. There are many other potential applications such as rapid peptide or protein hydrolysis as well as spores breaking to release their DNA.

The heating of the droplet was done through the glass and oil surrounding the droplet. The small droplet shape minimized the temperature gradient through the droplet, thus fulfilling the last condition for a superheated reactor. The VRC, used in this work, was formed by a 200 nl sample volume of fluorescein, covered with 600 nl of M5904 mineral oil (Sigma, Ltd.) and placed on an 170 μm thick hydrophobic/oleophobic microscope cover slip.

We used the chemical vapor deposition method to silanize the glass cover slips. The glass was first cleaned in a boiling H_2SO_4/H_2O_2 (piranha solution) mixture for 20 min, then rinsed in deionized water, and dried by the flow of nitrogen. Glass treatment in a piranha solution also formed –OH groups at the surface preparing it for subsequent step of silanization. The glass was then placed into a room temperature vacuum oven with 50 μl of a fluorosilane solution such as (heptadecafluoro-1,1,2,2-tetrahydrodecyl)trimethoxysilane (FAS17) or (1H,1H,2H,2H-perfluorooctyl)trichlorosilane (FOTS) both from Gelest, Inc. The oven was closed and evacuated by a conventional oil rotary pump into pressure smaller than 0.1 Torr and flushed three times with nitrogen. We then increased the temperature inside the oven while the pump was still running. Once the temperature reached 150 °C, we kept the system steady for 20 min. After that we flushed it again three times with nitrogen, switched off the pump, vented it with nitrogen, and took the glass out. We achieved a self-assembly monolayer of a fluorosilane with reproducible contact angle between 105° (FAS17) and 115° (FOTS).

The glass was then placed on a micromachined silicon chip, integrated with a thin film heater as well as the temperature sensor both made of an Au/Cr sandwich as described earlier.[4] The heating rate dT/dt of the heater is function of the power dissipation P and thermal capacitance H of the material to be heated

$$\frac{dT}{dt} = \frac{P}{H}, \tag{1}$$

where $P = \frac{V^2}{R}$ and V is voltage across the heater and R its resistance.

Resistance of the heater in our previous work[4,5] was 110 Ω and 141 Ω for older and newer work respectively, and we used voltage pulses with amplitude between 12 V and 16 V as power supply. The heating rate of the heater itself increased from 50 °C/s (Ref. 4) to 175 °C/s (Ref. 5) due to the adoption of a simplified shape of the heater with a single donut shape. The double donut shape has superior temperature uniformity but the single donut shape-based heater has a smaller heat mass, making it significantly faster, which was more important. The system thermal time constant τ dropped from 1.74 s to 0.28 s. Once the device was equipped with the VRC, the system was also much faster due to smaller thermal mass of the sample/oil system as its volume dropped from 1 μl/5 μl to 0.1 μl/1.1 μl.

The device presented in this article is terminated with a single donut shape with heater and sensor resistance values of ~90 Ω and ~250 Ω, respectively. The heater was powered with pulses of 20 V amplitude, resulting in a heating rate of 650 °C/s. The VCR volume also dropped to 0.2 μl of sample and 0.6 μl of oil (see the device in Fig. 2).

The chips were soldered on to a printed circuit board (PCB) using a simplified flip-chip technique. The conductance $G = 1.7\,\mathrm{mW\,K^{-1}}$ of the VRC were extracted using a single power pulse method.[6] The value of the thermal time constant τ was measured to be 0.17 s and based on the following equation:

$$\tau = H/G, \tag{2}$$

the value of thermal capacitance was calculated to be $H = 9.8\ \mathrm{mJ\,K^{-1}}$.

We also performed a numerical simulation of the VCR response to a heat pulse (emulating silicon heater behavior). For this, the finite element method (FEM) was used. To simplify very complex physics related to boiling, such as nucleation and vaporization, we considered both oil and water as solid bodies. Thus, all thermal effects were due to conduction and all the problematic thermal effects related to convection were eliminated. To obtain results of a high accuracy, a regular finite element mesh using hexahedral elements was created. The FEM package ANSYS was used to create the numerical model and carry out the simulation. A transient thermodynamic analysis with a stopping time of 20 s and with a time step of 0.1 s was performed. Results of numerical simulation shown graphically thermal distribution in the VRC for time equal to 0.2 s, 0.4 s, 0.6 s, 0.8 s, 1.0 s,

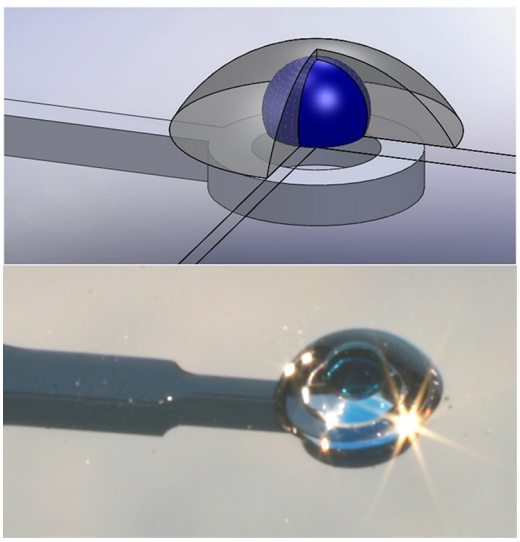

FIG. 2. (Top) Schematic drawing of the VRC with a miniaturized "hotplate" underneath, represented by a silicon ring. The ring-shaped silicon support is integrated with the heater and the temperature sensor made of thin gold film. A silicon cantilever connects the ring to a frame providing mechanical, thermal, and electrical connection with the PCB. The sample (represented by the blue sphere) is covered with mineral oil and placed on a thin glass substrate. (Bottom) A photograph of a fabricated silicon system with VRC consisting of 200 nl sample (blue color) covered with 600 nl of mineral oil, placed on an 170 μm thin microscope cover slip.

and 2 s, respectively, are shown in Fig. 3. A multimedia view (Fig. 3) is shown demonstrating simulated temperature distribution from 0 s to 15 s with a time difference between simulations from 0.2 s to 1 s. The verification of the model by contact measurement of the sample temperature was not possible. Any solid state temperature sensor inserted into the sample will add thermal mass and connecting wires will increase thermal conductivity, thus affecting the measurement precision. Due to the small volume, the only option is a non-contact measurement such as infrared-based (IR).[7] This is a recently introduced photothermal,[8] based on thermochromatic dye,[9] measurement of sample fluorescence amplitude either of fluorescein,[10] or two point temperature measurement based on DNA in the presence of intercalating dye.[11] In this paper, we extracted the sample temperature in fluorescence amplitude of the most commonly used fluorescent dye fluorescein.[10] It was a convenient method as the hardware with optics for subsequent molecular biology steps had built-in the fluorescent measurement system matching excitation and emission spectra of fluorescein.

We used an X-Cite 120 PC (EXPO Photonic Solution, Inc.) 120 W metal halide short arc lamp for sample illumination after being filtered by a blue filter from fluorescein isothiocyanate (FITC) filter set model 49002 (Chroma Technology Corp.). The emitted light was filtered by a green filter from the sample filter set, detected by a photomultiplier module H5784–20 (Hamamatsu, K.K.) and recorded by an oscilloscope.

We placed a sample of fluorescein with a concentration of 10 μM into the VRC and exposed it to a heat pulse of 155 °C. The heater temperature was controlled by a LabView program using the pulse-width modulation (PWM)

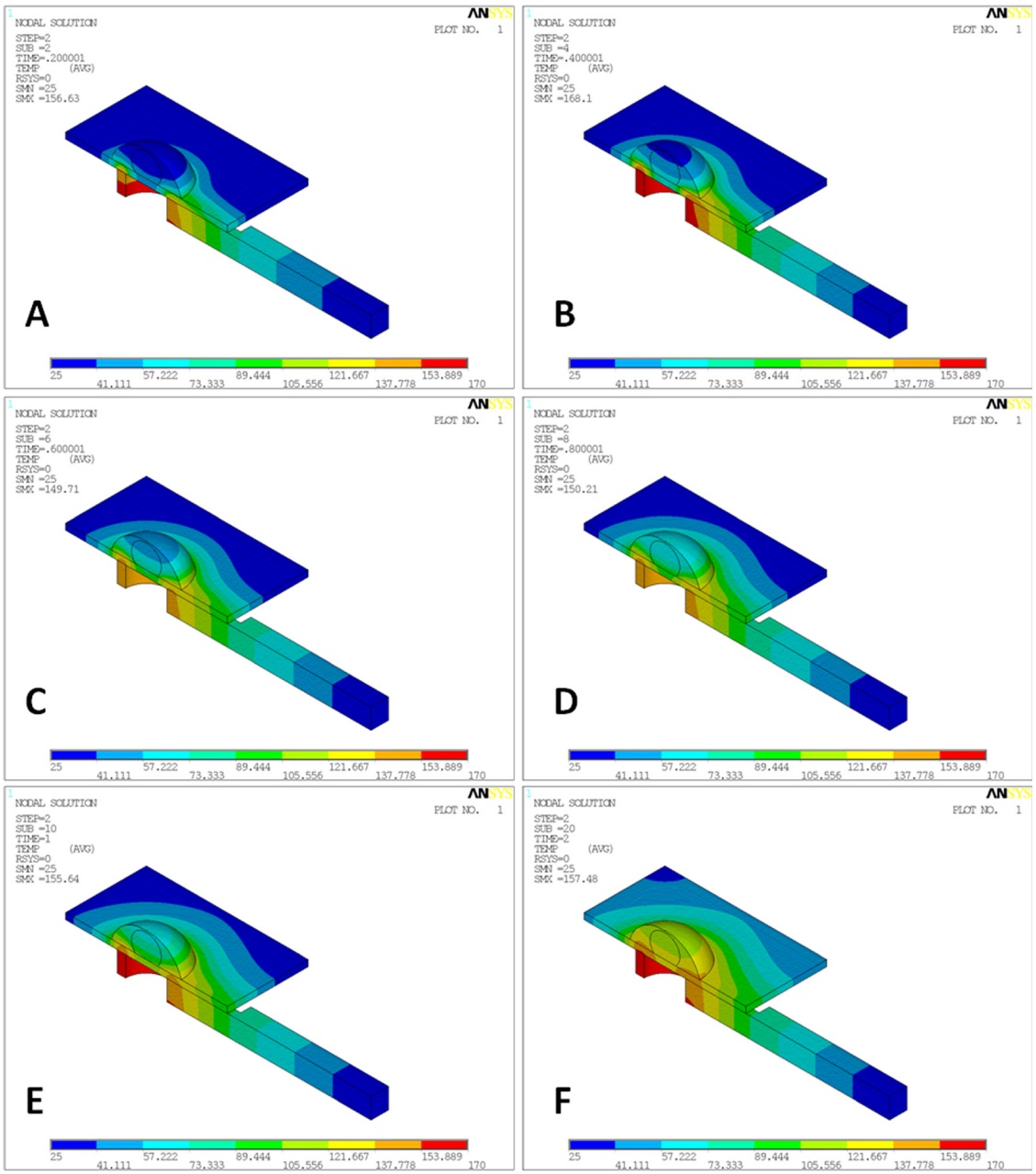

FIG. 3. FEM transient thermal analysis of the VRC performed by ANSYS FEM software with time resolution of 0.1 s. Temperature distribution within the model is shown at (a) 0.2 s, (b) 0.4 s, (c) 0.6 s, (d) 0.8 s, (e) 1.0 s, and (f) 2.0 s are shown here. (Multimedia view) [URL: http://dx.doi.org/10.1063/1.4905851.1]

principle with a proportional integration differentiation (PID) control in a closed feedback loop. One should note that optimizing the PID constants to achieve a fast yet stable control system was not an easy task. We did it purely empirically. First, we set the I and D values to zero, while gradually increased P until the system started to be unstable. Then, we have decreased P a little and started to optimize the I value. Here, in spite of previous work, we also used small value of D to make our system faster.

The temperature sensitivity of fluorescence amplitude was assumed to follow polynomial function of second order[10]

$$F = \alpha + \beta T + \gamma T^2, \tag{3}$$

where α, β, and γ are coefficients of the polynomial function.

Temperature T as function of time, t, from second order system can be described by the following equation:

$$T = A_1 + A_2 \exp\left(-\frac{t - t_0}{\tau_1}\right) + A_3 \exp\left(-\frac{t - t_0}{\tau_2}\right), \tag{4}$$

where A_1, A_2, and A_3 are constants related to the measurement system, t_0 is the time when the power is switched on, and τ_1 and τ_2 are thermal time constants of the heater and sample, respectively. As mentioned before, the heater temperature as a function of time is almost a step function. Thus, Eq. (4) can be simplified into an exponential function of the first order. With these assumptions, we derived coefficients of the polynomial function (3) by curve fitting of fluorescence amplitude as a function of time shown in Fig. 4.

Once the temperature sensitivity of fluorescence amplitude was known, the VCR was repeatedly heated to different temperatures in the range of 100 °C and 200 °C for 10 s and let to cool for 15 s.

A typical set of results is shown in Fig. 4 with a sample heating to 155 °C. The red line/squares show measured sample temperature, the light green line/circles sample temperature simulated by FEM. The purple line/down triangles are the fluorescence measurements. The extracted temperature from the fluorescence amplitude is represented by the dark green line/up triangles. There are several outcomes worth pointing out. First, the heater has an incredible heating rate of 613 °C/s, resulting in achieving the desired heater temperature of 155 °C in 0.2 s. The heating rate of the VRC was determined by a numerical differentiation of the sample temperature with respect to time resulting in over 229 °C/s.

The sample cooling rate was also remarkably high with a value of $-45\,^{\circ}\mathrm{C\ s^{-1}}$. Interestingly, the sample temperature derived from the fluorescence showed that the actual sample temperature increase is significantly faster than the one predicted by the FEM simulation. This measurement—simulation discrepancy is most likely caused by the convection of the droplet contents during heating which casts doubt on a FEM simulation precision. Nevertheless, the FEM can still be considered a limiting case with assumption of no fluid motion. In reality, the system heat transfer is significantly faster than the one predicted by FEM. Using an optical microscope, we indeed observed that the water sample does move violently within the temperature when the VRC is

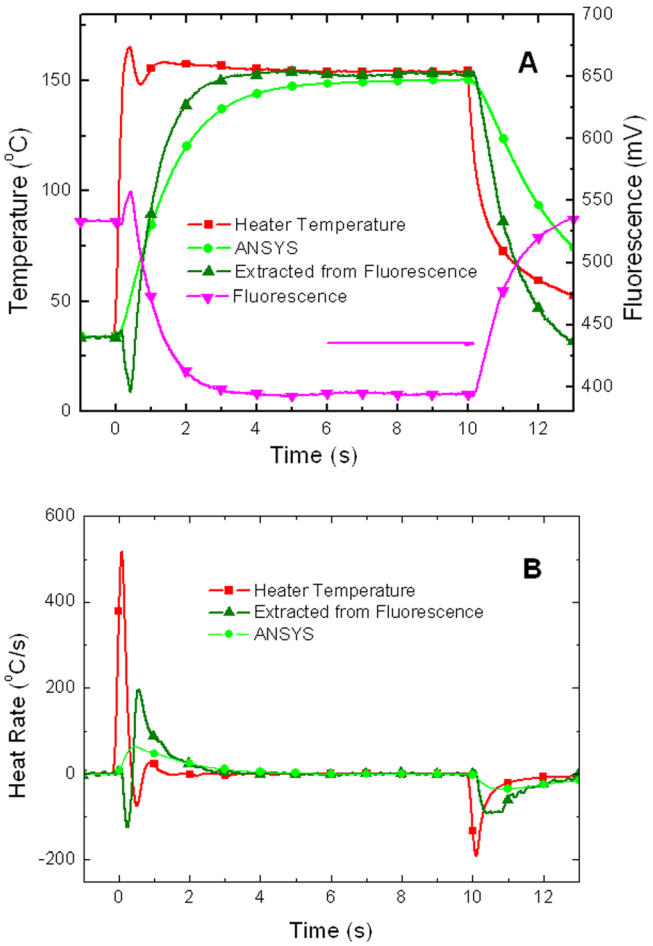

FIG. 4. (a) The heater temperature (red squares) and fluorescence amplitude (down purple triangles) as a function of time during heating the sample to 155 °C and cooling back to room temperature. The temperature extracted from captured fluorescence amplitude (green up triangles) is also shown. Desired temperature of the heater was achieved in 0.2 s, corresponding to the heating rate of 650 °C/s. (b) Numerical derivation of the temperatures with respect to time showing remarkable heating rated of the heater itself (613 °C/s) as well as of the VRC (229 °C/s). The colors are symbols are the same as in (a).

raised to 100 °C or higher. Finally, we observed that there is ~1.5 s lag between the sample and heater temperature. This lag would explain why the shortest denaturation time in our previous PCR protocol[5] was 1.5 s. Anything shorter than that would produce non-reproducible results.

We extracted thermal time constants from the experiments shown in Fig. 4 using a non-linear curve fitting by Levenberg-Marquardt method in the software Origin version 7.5 (Microcal, Inc.). As mentioned above, we use PID system for temperature regulation. At the beginning of the heat pulse, the heater temperature followed an almost step function. Thus, its time constant was not applicable for sample heating. The cooling was done naturally by switching the heater off so both the heater and the sample time constant played their role. All extracted parameters from the FEM model, electrical, and optical measurements are in Table I.

Thermal time constant τ_1 extracted from the amplitude of sample fluorescence is twice as fast as the one extracted from the FEM simulation. Interestingly, we found that the system behavior is predominantly of first order, as shown by low value of A_2/A_1 ratio. It means that the heater thermal

TABLE I. The extracted values of time constants from measured and simulated (FEM) results. The first number represents the thermal time for heating and the second one for cooling. The ratio between constant A_1 and A_2 shows which time constant controls the system behavior. Please note that the time constants τ_1 and τ_2 as well as their ratio could not be determined for the heating of the heater due to the implementation of the PID regulation.

	Heater temperature	Optical	FEM
τ_1 (s)	N.A./3.35	0.68/1.05	1.20/2.30
τ_2 (s)	N.A./0.53	3.76/N.A.	0.48/0.13
Ratio A_2/A_1	N.A./1.05	0.015/N.A.	0.17/0.98

parameter played a dominating role, compared to the heat transfer via glass cover slip.

We ran a set of experiments with pulse temperatures of up to 200 °C. The water sample was mostly stable but at that temperature, the oil started to evaporate at high rate, changing the thermal properties of the VRC. The mineral oil 9405 could be changed into another material with a lower saturated vapor pressure. This would allow increasing the VRC temperature even higher.

At a temperature of 200 °C, we used only 20% duty cycle of the PWM power supply system. The silicon heater temperature is linearly proportional to its thermal conductivity G and the dissipated power. The value of G is a fixed value, done by the cross-section of the silicon beam, its length, and material properties of silicon. We could increase the duty cycle of the PWM to 100%, which should increase the heater temperature up to ~800 °C with assumption of neglecting the thermal radiation losses. In reality, it is not possible to increase temperature so much due to other limiting factors such as device materials and the chance of damaging the chip. Nevertheless, using different oil for the VRC would significantly increase the maximum achievable sample temperature.

We have proposed and tested a simple method for superheating water samples. We have also demonstrated that it is possible to stabilize a water droplet at 200 °C temperature without boiling. This superheated droplet could be used to break a bacteria spore shell and thus release DNA for its subsequent detection.[3] The safety concern in case a superheated droplet starts boiling is negligible for small volumes. The small scale and the reproducibility of superheating as shown here make this method very interesting for a wide variety of small volume applications, such as life sciences applications. Volume greater than 100 nl can be handled by hand using a conventional pipette making the system convenient. Once the superheating is performed, the sample can be moved by pipetting into another station such as real-time PCR for DNA detection, Agilent's Bioanalyzer for capillary electrolysis, etc. Protein chemistry, nucleotides chemistry, carbohydrate chemistry, and sterilization could also benefit from well-defined short pulses of high water temperature. Other examples include crystallization, chemical synthesis, and fluorescence labeling reaction.

P. Neužil would like to acknowledge partial support by the project CEITEC CZ.1.05/1.1.00/02.0068. The authors would like to show their appreciation for earlier technical help by J. Pipper and J. Reboud and to M. Neužilová for her editorial work.

[1]D. Zahn, Phys. Rev. Lett. **93**(22), 227801 (2004).
[2]D. J. Miller, S. B. Hawthorne, A. M. Gizir, and A. A. Clifford, J. Chem. Eng. Data **43**(6), 1043 (1998).
[3]A. Pribylka, A. V. Almeida, M. O. Altmeyer, J. Petr, J. Sevcik, A. Manz, and P. Neuzil, Lab Chip **13**(9), 1695 (2013).
[4]P. Neuzil, J. Pipper, and T. M. Hsieh, Mol. BioSyst. **2**(6–7), 292 (2006).
[5]P. Neuzil, C. Zhang, J. Pipper, S. Oh, and L. Zhuo, Nucleic Acids Res. **34**(11), e77 (2006).
[6]X. Gu, G. Karunasiri, G. Chen, U. Sridhar, and B. Xu, Appl. Phys. Lett. **72**(15), 1881 (1998).
[7]H. A. Gronlund, C. Lofstrom, J. B. Helleskov, and J. Hoorfar, Food Anal. Methods **3**(2), 116 (2010).
[8]M. N. Slyadnev, Y. Tanaka, M. Tokeshi, and T. Kitamori, Anal. Chem. **73**(16), 4037 (2001).
[9]A. Seeboth, D. Lotzsch, R. Ruhmann, and O. Muehling, Chem. Rev. **114**(5), 3037 (2014).
[10]D. Ross, M. Gaitan, and L. E. Locascio, Anal. Chem. **73**(17), 4117 (2001).
[11]P. Neuzil, F. Cheng, J. B. Soon, L. L. Qian, and J. Reboud, Lab Chip **10**(20), 2818 (2010).